Desalination and Water Treatment
www.deswater.com

doi:10.5004/dwt.2018.21717

107 (2018) 147–154
March

Carbon dots as fluorescent probe for selective and sensitive detection of cerium (III) ion

Yinyin Wang[a], Fanyong Yan[a,*], Depeng Kong[a], Fanlin Zu[a], Zhangjun Bai[a], Jinxia Xu[a], Li Chen[b,*]

[a]*State Key Laboratory of Separation Membranes and Membrane Processes/National Center for International Joint Research on Separation Membranes, School of Environmental and Chemical Engineering, Tianjin Polytechnic University, Tianjin 300387, China, email: 18556375318@139.com (Y. Wang), Tel. +86 2283955766, Fax +86 2283955766, email: yanfanyong@tjpu.edu.cn (F.Y. Yan), 1126070345@qq.com (D. Kong), 609119111@qq.com (F. Zu), 18396544699@163.com (Z. Bai), xujinxairuth@163.com (J. Xu)*
[b]*Institute of Separation Material and Process Control, School of Material Science and Engineering, Tianjin Polytechnic University, Tianjin 300387, China, Tel. +86 2283955766, Fax +86 2283955766, email: Chenlis@tjpu.edu.cn (L. Chen)*

Received 20 May 2017; Accepted 19 November 2017

ABSTRACT

Carbon dots (CDs) as a new class of carbon nano materials have attracted considerable attention owing to its outstanding merits including excellent water solubility, good bio compatibility and high photo stability. Herein, a simple and effective method was designed to detect Cerium (III) (Ce^{3+}) based on fluorescence quenching of CDs. The fluorescent CDs were synthesized using traditional Chinese medicine residues as the carbon source by a simple and one-step reflux method. The prepared CDs have a bright blue fluorescence and a relatively high quantum yield of 32%. The fluorescence of CDs can be efficiently quenched by the addition of Ce^{3+}. Moreover, a good linear relationship was obtained between the degree of fluorescence quenching and the concentration of Ce^{3+} in the range of 100–250 μM, with a detection limit of 2.51 μM. This probe also showed high selectivity over other interferential cations. It is demonstrated that the CDs based fluorescent probe can be used to detect Ce^{3+} in real water samples.

Keywords: Carbon dots; Cerium (III); Fluorescence probe; Fluorescence quenching; Real water samples

1. Introduction

The rare earth elements (REE), also referred to as the lanthanide's, are a series of elements with atomic numbers between 57 and 71 [1–3]. They are widely used in all major applications in nuclear energy, metallurgy, agriculture, electronics, medical, and chemical engineering due to their specific physical and chemical properties [4–8]. Among the REE, Cerium is the most abundant element, averaging 22 mg kg^{-1} in various soils worldwide [9,10]. It exists dominantly in a trivalent ion (Ce^{3+}). The increasing use of Ce^{3+} application in functional materials and metallurgical areas leads to the researchers study its effects on the environment and human health [11,12]. From a biological and a toxicological point of view, Ce^{3+} affects the physiological activities of organism [13]. When it is inhaled with air, Ce^{3+} can cause various diseases such as lung embolisms or threatens the liver [14,15]. Therefore, the development of rapid and sensitive analysis methods for the determination of Ce^{3+} is of significant interest.

In the past ten years, various approaches have been developed in literature for the effective determination of Ce^{3+}, such as inductively coupled plasma atomic emission spectroscopy (ICP-AES), including inductively coupled plasma mass spectrometry (ICP-MS), electro thermal atomic absorption, spectrofluorometry, and neutron activation analysis [16–21]. However, these methods suffer from the expensive instruments, complicated processes and may be unavailable in some areas. In fact, superior methods for the detection of Ce^{3+} are still greatly needed.

*Corresponding author.

The tremendous progress in the research of different functional groups based nano materials brings the opportunities for optical detection Ce^{3+} by considering their fast response, high sensitivity and selectivity and cost effectiveness [22,23]. Although Ce^{3+} is similar characteristics and it is difficult to separate from REE. This encourages the development of optical detection of Ce^{3+} by using nano materials. The coordination chemistry of REE with O- and N-donor ligands has advanced because of the fact that steric factors can be optimized with the ligand set Ce^{3+} contraction by choosing the best size of REE [24,25]. This has led to the development of an optical detection and recovery of Ce^{3+} with nano materials using functional discolor or fluorescence group ligand.

As a new member of the nano materials family, fluorescent carbon dots (C-dots) are small carbon nano particles with sizes below 10 nm, and have many fascinating advantages including excellent water solubility, good bio compatibility, low cytotoxicity, speed response, high selectivity and sensitivity at cost-effectiveness [26–31]. Currently, detection of Ce^{3+} using CDs in the solvent is still rare, all of them are metal ions such as Hg^{2+}, Fe^{3+}, Cu^{2+}, Pb^{2+}analysis fluorescent probes [32–35]. Therefore, development of sensing CDs as per the requirement of determination Ce^{3+} from REE is yet issue for scientists.

In this work, we report a highly sensitive nano sensor based on CDs for detection of Ce^{3+} by fluorescence spectrum. The CDs were synthesized from traditional Chinese medicine residues through a simple sodium hydroxide-assisted reflux method. This probe can be employed for the sensitive and selective detection of Ce^{3+} by fluorescence turn-off. The obtained CDs show excellent linear relationship towards Ce^{3+} in the concentration range from 100–250 μM with a detection limit of 2.51 μM. The mechanism was also discussed in paper. Furthermore, CDs can be applied for the selective determination of Ce^{3+} in water samples. To our knowledge, we report a fluorescence spectral sensing method for the detection of Ce^{3+} based on CDs for the first time. This probe provides a simple and inexpensive method for detecting Ce^{3+}.

2. Experimental

2.1. Chemicals and apparatus ETH

Sodium hydroxide (96.0%), hydrochloric acid (36.0–38.0%) and ethanol (99.7%) were purchased from Tianjin Guangfu chemical reagents Co., Ltd. (Tianjin, China). The traditional Chinese medicine residues were obtained from our school hospital (Tianjin, China). All the other chemicals were analytical grade and used as received. Deionized water by our own school was used throughout the experiments (Tianjin, China). Phosphate buffered solution (10 mM) was prepared by using a mixture Na_2HPO_4 and KH_2PO_4 (purchased from Tianjin yongda chemical reagent Co., Ltd) (Tianjin, China). The solutions of metal ions were prepared from $NaNO_3$ (99.0%), KNO_3 (99.0%), $MgSO_4$ (99.0%), $Ca(NO_3)_2$ (99.5%), $Ba(NO_3)_2$ (99.0%), $Ce(NO_3)_3$ (99.0%), $Cr(NO_3)_3$ (98.5%), $Mn(NO_3)_2$ (99.5%), $Fe(NO_3)_3$ (98.5%), $Co(NO_3)_2$ (99.0%), $Ni(NO_3)_2$ (98.0%), $PdCl_2$ (98.5%), $CuCl_2$ (99.5%), $AgNO_3$ (99.8%), $Zn(NO_3)_2$ (99.5%), $Cd(NO_3)_2$ (99.0%), $Hg(NO_3)_2$ (98.0%), $Al(NO_3)_3$ (99.0%), $Ga(NO_3)_3$ (98.5%), $Pb(NO_3)_2$ (99.0%) and $Sr(NO_3)_2$ (98.8%) (purchased from Tianjin Kemiou Chemical Reagent Co., Ltd) (Tianjin, China).

Transmission electron microscopy (TEM) measurements were performed on an H-7650 electronic microscope of HITACHI from Japan (Shanghai, China). The Fourier transform infrared spectroscopy (FTIR) spectra were recorded on a TENSOR37 Fourier-transform infrared spectrometer from Tianjin Gangdong Scientific and Technological Development Co., Ltd (Tianjin, China). The X-ray photo electron spectroscopy (XPS) spectra measurements were performed on an X-ray photo electron spectroscopy (EDAX, GENESIS 60S). UV–vis absorption spectra of the samples were recorded on a Purkinje General TU-1901 UV–vis spectrophotometer from Beijing Purkinje General Instrument Co., Ltd (Beijing, China). Fluorescence emission spectroscopy was carried out on an F-380 fluorescence spectrophotometer from Tianjin Gangdong Scientific and Technological Development Co., Ltd (Tianjin, China). A PHS-3W pH meter (Shanghai Lida instrument factory) was utilized to measure the pH values of aqueous solutions (Shanghai, China). The fluorescence imaging was observed under an Olympus IX71 inverted fluorescence microscope from Japan with a 20× objective lens (Beijing, China).

2.2. Synthesis of CDs

CDs were synthesized through a reflux method according to the reported procedure with some changes [36]. The traditional Chinese medicine residues (2 g) were added into 0.1 M sodium hydroxide (50 mL) under magnetic stirring. The solution became brown gradually after refluxing for 8 h at 120°C. After cooling down, the insoluble precipitate in the solution was removed by extraction filtration and centrifugation. Then the obtained solution was neutralized (pH = 7.0) by 0.1 M hydrochloric acid. Then the CDs solution was further purified through dialyzing with a dialysis tube (Mw = 3000) against doubly distilled water for 3 d. Eventually, pure CDs were obtained by rotary evaporation and freeze drying. The resulting powder was dispersed in distilled water at a concentration of 1 mg mL^{-1} for further use.

2.3. Quantum yield measurement

The fluorescence quantum yield was determined by slope method by the reference of quinine sulfate: compared the integrated photoluminescence intensity (λ_{ex}= 360 nm) and the absorbance value (several values gave the curve) of the CDs samples with that of the references. Then used the equation: $\phi_x = \phi_{st}(K_x/K_{st})(\eta_x/\eta_{st})^2$, where ϕ is the fluorescence quantum yield, K is the slope determined by the curves and η is the refractive index. The subscript "st" refers to quinine sulfate and "x" refers to the CDs. For these aqueous solutions, $\eta_x/\eta_{st} = 1$. So, the equation was simplified to: $\phi_x = \phi_{st}(K_x/K_{st})$.

2.4. Fluorescence assay of Ce^{3+}

Firstly, various metal ions solution of a concentration of 2 mM were prepared, including $NaNO_3$ (99.0%), KNO_3 (99.0%), $MgSO_4$ (99.0%), $Ca(NO_3)_2$ (99.5%), $Ba(NO_3)_2$

(99.0%), $Ce(NO_3)_3$ (99.0%), $Cr(NO_3)_3$ (98.5%), $Mn(NO_3)_2$ (99.5%), $Fe(NO_3)_3$ (98.5%), $Co(NO_3)_2$ (99.0%), $Ni(NO_3)_2$ (98.0%), $PdCl_2$ (98.5%), $CuCl_2$ (99.5%), $AgNO_3$ (99.8%), $Zn(NO_3)_2$ (99.5%), $Cd(NO_3)_2$ (99.0%), $Hg(NO_3)_2$ (98.0%), $Al(NO_3)_3$ (99.0%), $Ga(NO_3)_3$ (98.5%), $Pb(NO_3)_2$ (99.0%) and $Sr(NO_3)_2$ (98.8%). In a typical detection experiment, 0.2 mL CDs (1 mg mL^{-1}) solution was added into a certain amount of metal ions (0.2 mL) solution to form a 10 mL clear solution with water. After mixing completely and maintained for 30 min, fluorescence measurements were carried out at the excitation wavelength of 360 nm with the excitation and emission slit width of 5 and 10 nm. All samples were prepared at room temperature.

3. Results and discussion

3.1. Structural and optical characterization of CDs

The CDs were prepared by the reflux treatment of traditional Chinese medicine residues with sodium hydroxide, then a yellow brown solution was obtained. The morphology and particle size of the obtained CDs were determined by TEM. The TEM image demonstrates that CDs are well dispersed and spherical in shape as shown in Fig. 1. The CDs are mainly distributed in the range of 4–10 nm with an average size about 8 nm. The FTIR spectrum was tested to reveal the surface functional groups of CDs as shown in Fig 1b. The bands at 3404 and 1124 cm^{-1} are corresponds to the stretching vibrations of O-H and C-O, showing the presence of hydroxyl and other oxygen-containing functional groups. The stretching vibration bands of N-H at 3133 cm^{-1} and C-N at 1400 cm^{-1} indicate the existence of amino-containing functional groups. The FTIR spectrum also displays the absorption bands of C-H at 3001 cm^{-1} and C=C at 1602 cm^{-1}.

Then XPS was investigated to provide further evidence for the components and the surface functional groups of the CDs. The three typical strong peaks at 285, 403 and 532 eV as shown in Fig. 2a are attributed to C1s, N1s and O1s, respectively. The C1s spectrum shows two representative peaks at 284.8 eV and 288.2 eV, which are from C-C and N-C=O bands. The N1s can be resolved into two carbon states at 401 eV and 403 eV, which are attributed to N-H and N-C=O, respectively. The enlarged region of O1s reveals the signals of C-OH at 532.8 eV and N-O at 534 eV. All these FTIR and XPS results demonstrate that the prepared CDs contain functional groups with oxygen and nitrogen elements.

The optical properties were explored by UV-vis and fluorescence spectra as shown in Fig. 3. The absorption peak at 220 nm is attributed to the typical π–π* transition of aromatic sp^2 domains. The broad peak around 330 nm is due to n-π* transition of C=O [37]. The fluorescence emission peaks of CDs gradually red shift at increasing excitation wavelength from 300 nm to 400 nm. The strongest emission at 438 nm was obtained at the excitation wavelength of 360 nm. Therefore, 360 nm was chosen as the excitation wavelength for the following experiments. The quantum yield was calculated to be 32% with the quinine sulfate (54 % in 0.1 M H_2SO_4, λ_{ex} = 360 nm) as a reference material. The influence of pH on the fluorescence stability of the obtained CDs was investigated. As shown in Fig 3c, the fluorescence intensity at 438 nm increased gradually with the increase of the pH value of solution from pH 1.0 to 4.0 and then reached a maximum at pH 8.0. When the solution pH value continued to increase from pH 8.0 to 14.0, the fluorescence intensity decreased. So, pH 8.0 was chosen as the optimal pH for detecting the Ce^{3+}. It can be seen that the CDs have the high fluorescence intensity at pH 6.0–8.0, which indicates that the CDs would have a great potential application in biomedical field. There was no observation of coagulation particles even after being kept for 40 d, and the fluorescence intensity of CDs showed a negligible change as shown in Fig. 3d, which demonstrates that the synthesized CDs have good fluorescent stability.

3.2. The selectivity and sensitivity of CDs for Ce^{3+} detection

To investigate the selectivity of the CDs for Ce^{3+}, the fluorescence intensity of the CDs at 438 nm was measured after introducing of various metal cations. As listed in Fig. 4a,

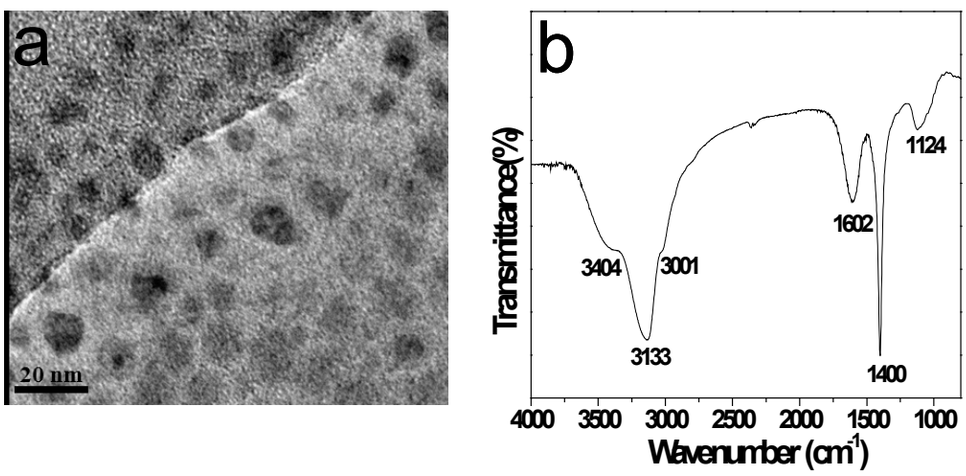

Fig. 1. TEM image of CDs, inset: the size distribution of CDs (a); FTIR spectrum of CDs (b).

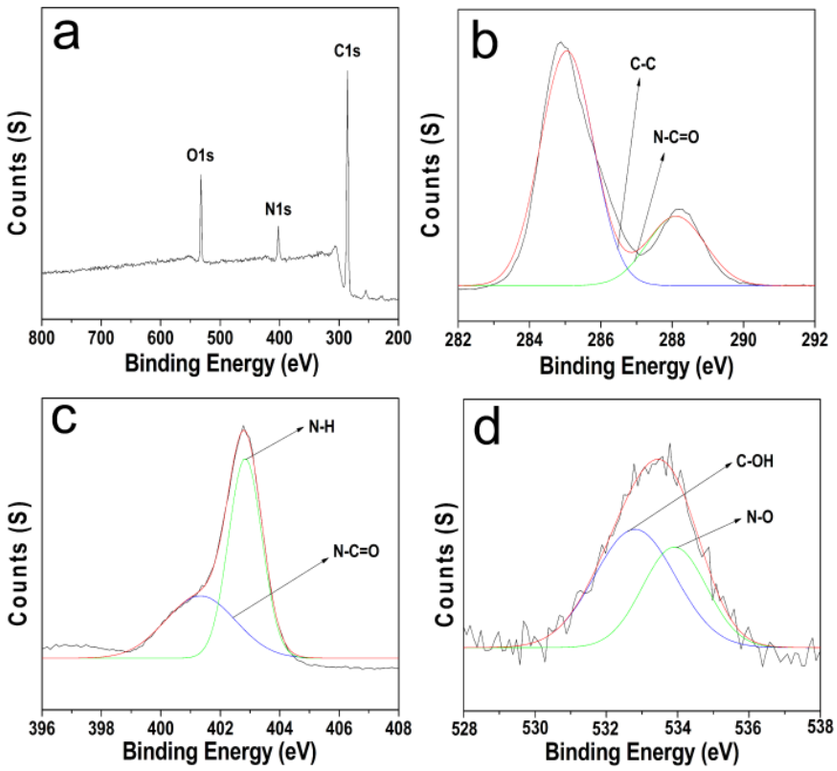

Fig. 2. XPS spectrum (a) and enlarged regions for C1s (b), N1s (c), O1s (d) of CDs.

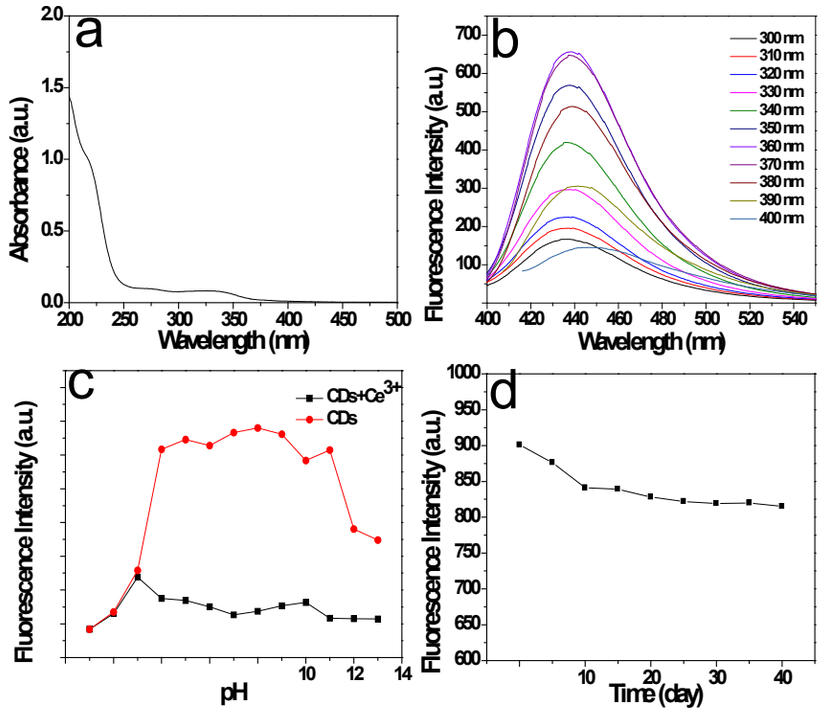

Fig. 3. Absorption spectra (λ_{ex} = 340 nm) of CDs (a); Fluorescence spectra (excitation wavelength from 300 to 400 nm in 10 nm increments) of CDs (b); Effect of the solution pH on the fluorescence intensity of the CDs(c); Stability of CDs (d).

except the addition of Ce^{3+} leading to obvious fluorescence quenching (75 %), the other metal ions show quite few effect on the fluorescent intensity of CDs, which confirmed that CDs could act as highly selective Ce^{3+} probe.

Fluorescence titration experiments were performed to investigate the sensitivity of the CDs toward Ce^{3+}. The result shown in Fig. 4a revealed that the fluorescence intensity changes of CDs at 438 nm were investigated with the increasing concentration of Ce^{3+}. Upon the addition of Ce^{3+}, significant fluorescence quenching at 438 nm can be observed. From the corresponding point plot shown in Fig. 4b, it can be clearly seen that the fluorescence signal decreased exponentially as the Ce^{3+} concentration ranging from 0 to 500 *μM. While, the fluorescence almost didn't change any more upon 400 μM, indicating that the CDs has reached saturation for* Ce^{3+} determination. F_0 and F are the fluorescent intensities of CDs in the absence and presence of Ce^{3+}, C is the concentration of Ce^{3+}. A good linear response towards Ce^{3+} concentration ranging from 100 to 500 μM was obtained shown in Fig. 4c. The limit of detection for the proposed probe was evaluated to be 0.22 μM using the formula: $3\sigma/s$, where σ is the standard deviation of blank signal (n = 6) and s is the slope of the calibration curve. In the contrast experiment, Ce^{3+} and the mixtures of Ce^{3+} and

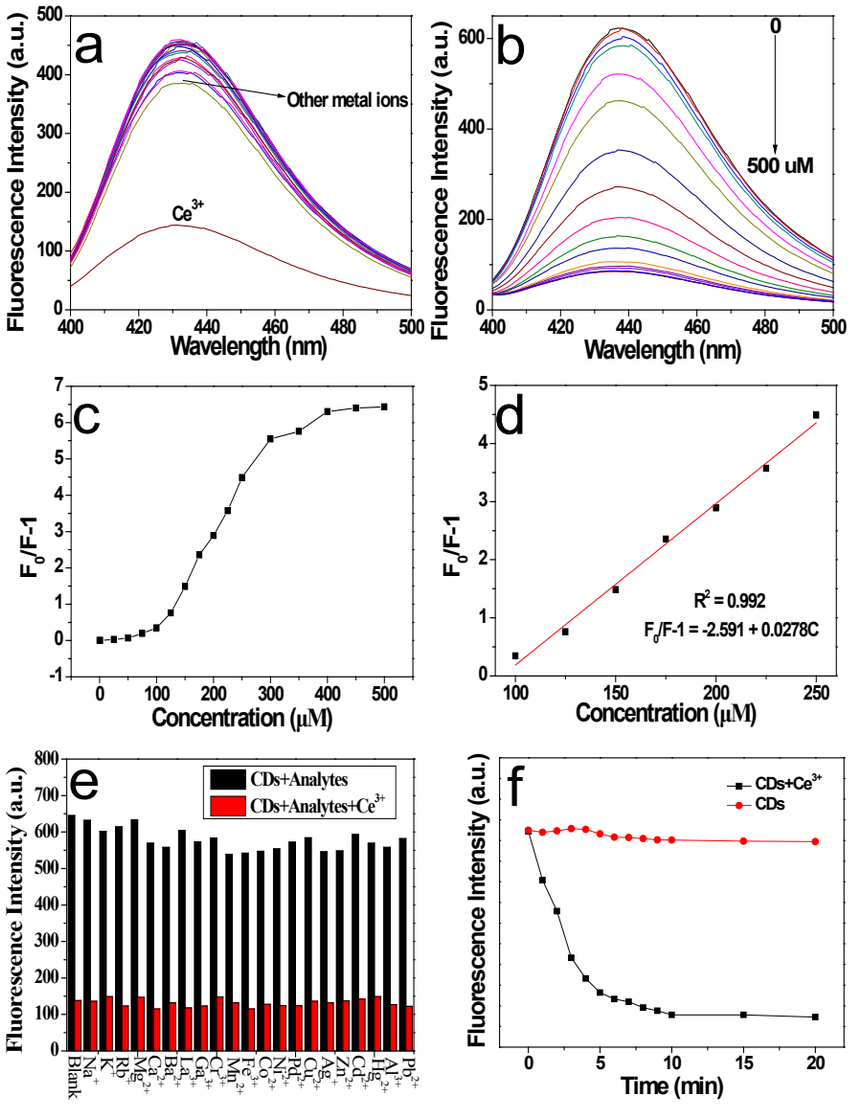

Fig. 4. Effect of various metal ions on the fluorescence intensity of CDs, the other metal ions including Na^+, K^+, Rb^+, Mg^{2+}, Ca^{2+}, Ba^{2+}, La^{3+}, Ce^{3+}, Cr^{3+}, Mn^{2+}, Fe^{3+}, Co^{2+}, Ni^{2+}, Pd^{2+}, Cu^{2+}, Ag^+, Zn^{2+}, Cd^{2+}, Hg^{2+}, Al^{3+}, Ga^{3+}, Pb^{2+} (a). Fluorescence emission spectra of CDs in the presence of different concentrations of Ce^{3+} (from 0 to 500 μM) (b); The corresponding point plot (c); The linear relationship of F_0/F-1 on the concentrations of Ce^{3+} in the range of 100–250 μM, (d); Fluorescence response of CDs in the presence of Ce^{3+} with the addition of competitive metal ions respectively (e). Reaction time on the fluorescence intensity of CDs in the absence (black) and presence (red) of Ce^{3+} (f).

the above mentioned metal ions were used to explore the fluorescence response of CDs.

For Ce^{3+} detection, one of the essential requirements was no interference or minor from various potentially competitive metal ions in the environment. Then, the competitive experiments were carried out by addition of 10 equiv. of Ce^{3+} to the CDs solutions in the presence of 50 equiv. of other metal ions. The result shown in Fig. 4e indicated that remarkable fluorescence quenching could be observed and the relative change of the emission intensity reached about 75 %, which confirms the remarked selectivity of CDs for Ce^{3+} in water.

To understand the response rate of the fluorescence signal of CDs to Ce^{3+}, the time-dependent fluorescence changes were evaluated. As shown in Fig. 4f, a remarkable fluorescence quenching of CDs was observed within 5.0 min of contact time. This suggests that Ce^{3+} initially quenches the fluorescence of CDs by binding to the surface groups of CDs (Fig. 6), which affects the surface states of CDs and results in the charge transfer from CDs to Ce^{3+}. Following this, the fluorescence quenching of CDs became slow until reaching a steady state at 5.0 min. A further increase of time did not lead to any further detectable quenching. Therefore, 5.0 min was selected as the optimum reaction time for Ce^{3+} detection to achieve low detection limit.

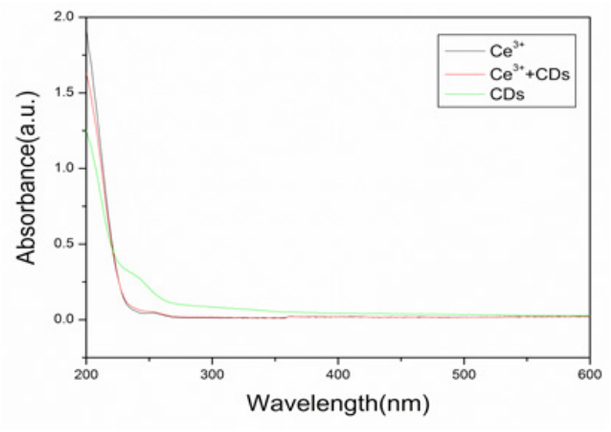

Fig. 5. The UV-vis absorption spectra of CDs under different conditions.

3.3. The mechanism for the detection of Ce^{3+}

The quenching mechanisms of CDs includes static quenching, dynamic quenching, FRER and IFE [38,39]. The Stern-Volmer plot fits a linear equation within the concentration range of 100–250 μM, indicating that only one type of these mechanisms occurs. Static quenching occurs when a nonfluorescent ground-state complex is formed through the interaction between CDs and quencher [40], so there will be a new absorption peak in the UV-absorption. But this process hasn't this phenomenon as shown in Fig 5a, so the quenching mechanism is not attributed to static quenching. FRET and IFE needs the spectrum overlap of the excitation or emission spectra of CDs and the absorption of quencher, this phenomenon doesn't occur in this quenching process because the Ce^{3+} hasn't the obvious absorption in the range of 250–450 nm, so the quenching mechanism is not attributed to FRET and IFE. Hence, the quenching mechanism is attributed to the dynamic quenching. The Stern-Volmer equation is $F_0/F\text{-}1 = -2.591 + 0.0278C$ as shown in Fig 4c. The constant of dynamic quenching is 0.0278 μM L^{-1}. It was further confirmed that the high selectivity of CDs to detection Ce^{3+} could be ascribed to the complexation between Ce^{3+} and the basic amino group and the hydroxyl portion in the surface of CDs, which facilitated the electron transfer from the CDs to the electron-deficient Ce^{3+} so as to shift the electron to the non-radiating decay path and quench the fluorescence emission of CDs (Fig. 6).

3.4. Detection of Ce^{3+} in real environmental samples

To verify the accuracy of the fluorescence detections methods, two water samples from natural water sources (tap water and ground water) were collected for determination of Ce^{3+}. Two water samples were stood for 24 h to precipitate and the supernatant was taken out for further analysis. In fluorescence spectra, no Ce^{3+} was found in the tap water and ground water samples. Then the water samples were spiked with two levels of 150 and 200 μM Ce^{3+} by the standard addition method. The recoveries were between 98.7% and 100.4% with low relative standard deviations (RSD) (Table 1). This result demonstrates that the prepared CDs are suitable for Ce^{3+} assay in environmental waters.

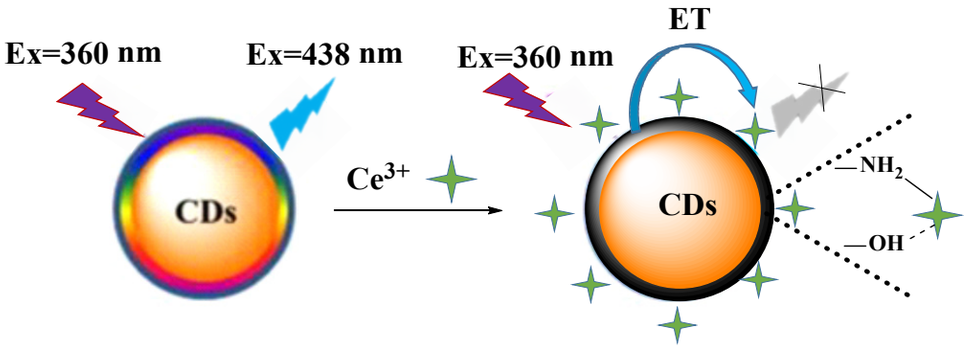

Fig. 6. Schematic illustration of CDs as fluorescent probes for the detection of Ce^{3+} through electron transfer process.

Table 1
Determination of Ce^{3+} spiked in real water samples (n = 3)

Sample used	Added (μM)	Found (μM)	R.S.D. (%, n = 3)	Recovery (%)
Tap water	150	149.5	1.9	99.9
	200	200.8	2.1	100.4
Ground water	150	148.0	2.9	98.7
	200	198.6	1.3	99.3

4. Conclusions

In summary, a simple and easy-to-prepare CDs based Ce^{3+} probe that contains the amino group and the hydroxyl unit was prepared and structurally characterized. It is worthy to note that the current probe can afford Ce^{3+}-selective fluorescence quenching and shows detection limits as low as the 0.22 μM level. Furthermore, the probe also exhibited high selectivity for Ce^{3+} over other metal ions. Analysis of fluorescence intensity shows that the procedure is a dynamic quenching process. Eventually, the CDs based probe also successfully applied to analyze environmental water samples with satisfactory recovery. CDs may be useful for application in toxicology and environmental science. This work provides a new method for the utilization of waste products.

Conflict of interest

The authors confirm that this article content has no conflict of interest.

Acknowledgements

The work described in this manuscript was supported by the National Natural Science Foundation of China (21374078, 51308390 and 51303132), The Science and Technology Plans of Tianjin (No. 15JCYBJC18100, 15JCTPJC59200, 15PTSYJC00250) and State Key Laboratory of Separation Membranes and Membrane Processes (Z1-201507).

References

[1] M.R. Awual, T. Kobayashi, H. Shiwaku, Y. Miyazaki, R. Motokawa, S.Suzuki, Y. Okamoto, T. Yaita, Evaluation of lanthanide sorption and their coordination mechanism by exafs measurement using novel hybrid adsorbent, Chem. Eng. J., 225 (2013) 558–566.
[2] H.T. Li, Z.H. Kang, Y. Liu, S.T. Lee, Carbon nano dots: synthesis, properties and applications, J. Mater. Chem., 22 (2012) 24230–24253.
[3] M.R. Awual, T. Kobayashi, Y. Miyazaki, R. Motokawa, H. Shiwaku, S. Suzuki, Y. Okamoto, T. Selective lanthanide sorption and mechanism using novel hybrid lew is base (n-methyl-n-phenyl-1,10-phenanthroline-2-carboxamide) ligand modified adsorbent, J. Hazard. Mater., 252–253 (2013) 313–320.
[4] Z. Yang, M.H. Xu, Y. Liu, F.J. He, F. Gao, Y.J. Su, H. Wei, Y.F. Zhang, Nitrogen-doped, carbon-rich, highly photo luminescent carbon dots from ammonium citrate, Nano scale, 6 (2014) 1890–1895.
[5] Y.X. Fang, S.J. Guo, D. Li, C.Z. Zhu, W. Ren, S.J. Dong, E. Wang, Easy synthesis and imaging applications of cross-linked green fluorescent hollow carbon nano particles, ACS Nano., 6 (2015) 400–409.
[6] J. Liu, Y. Liu, N.Y. Liu, Y.Z. Han, X. Zhang, H. Huang, Y. Lifshitz, S.T. Lee, J. Zhong, Z.H. Kang, Metal-free efficient photo catalyst for stable visible water splitting via a two-electron pathway, Science, 347 (2015) 970–974.
[7] V. Gupta, N. Chaudhary, R. Srivastava, G.D. Sharma, R. Bhardwaj, S. Chand, Luminscent graphene quantum dots for organic photo voltaic devices, J. Am. Chem. Soc., 133 (2011) 9960–9963.
[8] F.Y. Yan, D.P. Kong, Y.M. Luo, Q.H. Ye, Y.Y. Wang, L. Chen, Carbon nano dots prepared for dopamine and Al^{3+} sensing, cellular imaging and logic gate operation, Mater. Sci. Eng. C., 68 (2016) 732–738.
[9] M.R. Awual, M.M. Hasan, A. Shahat, M. Naushad, H. Shiwaku, T. Yaita, Investigation of ligand immobilized nano-composite adsorbent for efficient cerium(iii) detection and recovery, Chem. Eng. J., 265 (2015) 210–218.
[10] A.P. Jones, F. Wall, C.T. Williams, Rare earth minerals. Chemistry, origin and ore deposits, Mineral. Mag., 60 (1996) 853–853.
[11] F.W. Oehme, Toxicity of Heavy Metals in the Environment, Marcel Dekker, New York, 1979, 971.
[12] C. Dujardin, C. Mancini, D. Amans, G. Ledoux, D. Abler, E. Auffray, P. Lecoq, D. Perrodin, A. Petrosyan, K.L. Ovanesyan, LuAG: Ce fibers for high energy calorimetry, J. Appl. Phys., 108 (2010) 013510.
[13] J.M. Li, W.T. Wei, Catalytic kinetic spectrophotometric determination of cerium, J. Rare Earth., 28 (2010) 387–390.
[14] R. Filipi, K. Nesmerak, M. Rucki, Z. Roth, I. Hanzlikova, M. Tichy, Acute toxicity of rare earth elements and their compounds, Chem. Listy, 101 (2007) 793–798.
[15] N.A. Fitriyanto, M. Nakamura, S. Muto, K. Kato, T. Yabe, T. Iwama, K. Kawai, A. Pertiwiningrum, Ce^{3+}-induced exopolysaccharide production by Bradyrhizobium sp. MAFF211645, J. Biosci. Bioeng., 111 (2011) 146–152.
[16] M. Ayranov, J. Cobos, K. Popa, V.V. Rondinella, Determination of REE, U, Th, Ba, and Zr in simulated hydro geological leachates by ICP-AES after matrix solvent extraction, J. Rare Earth., 27 (2009) 123–127.
[17] Y. Hamajima, M. Koba, K. Endo, H. Nakahara, Determination of lanthanoids in Japanese standard rocks by radiochemical neutron activation method, J. Radioanal. Nucl. Chem., 89 (1985) 315–321.
[18] A.S. Amin, M.M. Moustafa, A.R.M. Issa, A rapid, selective and sensitive spectrophotometric method for the determination of Ce(III) using some bisazophenyl-b-diketone derivatives, Talanta, 44 (1997) 311–317.
[19] M. Eid, A. El-Brashy, F. Aly, W. Talaat, Spectro fluorometric determination of ketorolac tromethamine via its oxidation with cerium(IV) in pharmaceutical preparations and biological fluids, J. Aoac Int., 90 (2007) 941–947.
[20] V.K. Gupta, A.K. Singh, B. Gupta, A cerium(III) selective polyvinyl chloride membrane sensor based on a Schiff base complex of N, N`-bis [2- (salicylideneamino)ethyl]ethane-1,2-diamine, Anal. Chim. Acta., 575 (2006) 198–204.
[21] A. Garg, V. Susila, L.R. Kakkar, Spectrophotometric determination of cerium (IV) using potassium ferrocyanide as an analytical reagent, J. Indian Chem. Soc., 83 (2006) 626–628.
[22] A. Afkhami, T. Madrakian, A. Shirzadmehr, M. Tabatabaee, H. Bagheri, New Schiff base–carbon nano tube–nano silica–ionic liquid as a high performance sensing material of a potentio metric sensor for nano molar determination of cerium(III) ions, Sens. Actuators B: Chem., 174 (2012) 237–244.
[23] T.A. Ali, G.G. Mohamed, E.M.S. Azzam, A.A. Abd-Elaal, Thiol surfactant assembled on gold nano particles ion exchanger for screen-printed electrode fabrication. Potentio metric determination of Ce (III) in environmental polluted samples, Sens. Actuators B: Chem., 191 (2014) 192–203.
[24] M.R. Awual, T. Yaita, H. Shiwaku, Design a novel optical adsorbent for simultaneous ultra-trace cerium(III) detection, sorption and recovery, Chem. Eng. J., 228 (2013) 327–335.

[25] M.R. Awual, N.H. Alharthi, Y. Okamoto, M.R. Karim, E. Halim, M. Hasan, M.M. Rahman, M. Islam, A. Khaleque, C. Sheikh, Ligand field effect for Dysprosium (III) and Lutetium (III) adsorption and EXAFS coordination with novel composite nano materials, Chem. Eng. J., 320 (2017) 427–435.
[26] Z. Yang, M.H. Xu, Y. Liu, F.J. He, F. Gao, Y.J. Su, H. Wei, Y.F. Zhang, Nitrogen-doped, carbon-rich, highly photo luminescent carbon dots from ammonium citrate, Nano scale, 6 (2014) 1890–1895.
[27] Y.X. Fang, S.J. Guo, D. Li, C.Z. Zhu, W. Ren, S.J. Dong, E. Wang, Easy synthesis and imaging applications of cross-linked green fluorescent hollow carbon nano particles, ACS Nano., 6 (2015) 400–409.
[28] J. Liu, Y. Liu, N.Y. Liu, Y.Z. Han, X. Zhang, H. Huang, Y. Lifshitz, S.T. Lee, J. Zhong, Z.H. Kang, Metal-free efficient photo catalyst for stable visible water splitting via a two-electron pathway, Science, 347 (2015) 970–974.
[29] V. Gupta, N. Chaudhary, R. Srivastava, G.D. Sharma, R. Bhardwaj, S. Chand, Luminscent graphene quantum dots for organic photo voltaic devices, J. Am. Chem. Soc., 133 (2011) 9960–9963.
[30] F.Y. Yan, D.P. Kong, Y.M. Luo, Q.H. Ye, Y.Y. Wang, L. Chen, Carbon nano dots prepared for dopamine and Al^{3+} sensing, cellular imaging and logic gate operation, Mater. Sci. Eng. C, 68 (2016) 732–738.
[31] Z.M. Zhang, Y.P. Shi, Y. Pan, X. Cheng, L.L. Zhang, J.Y. Chen, M.J. Li, C.Q. Yi, Quinoline derivative-functionalized carbon dots as a fluorescent nano sensor for sensing and intracellular imaging of Zn^{2+}, J. Mater. Chem. B, 2 (2014) 5020–5027.
[32] F.Y. Yan, Y. Zou, M. Wang, X.L. Mu, N. Yang, L. Chen, Highly photo luminescent carbon dots-based fluorescent chemosensors for sensitive and selective detection of mercury ions and application of imaging in living cells, Sensor. Actuat. B-Chem., 192 (2014) 488–495.
[33] L.L. Zhu, Y.G. Yin, C.F. Wang, S. Chen, Plant leaf-derived fluorescent carbon dots for sensing, patterning and coding, J. Mater. Chem. C, 1 (2013) 4925–4932.
[34] S. Liu, J.Q. Tian, L. Wang, Y.W. Zhang, X.Y. Qin, Y.L. Luo, A.M. Asiri, A.O. Al-Youbi, X.P. Sun, Hydrothermal treatment of grass: a low-cost, green route to nitrogen-doped, carbon-rich, photo luminescent polymer nano dots as an effective fluorescent sensing platform for label-free detection of Cu(II) Ions, Adv. Mater., 24 (2012) 2037–2041.
[35] S.S. Wee, Y.H. Ng, S.M. Ng, Synthesis of fluorescent carbon dots via simple acid hydrolysis of bovine serum albumin and its potential as sensitive sensing probe for lead (II) ions, Talanta, 116 (2013) 71–76.
[36] A. Basu, A. Suryawanshi, B. Kumawat, A. Dandia, D. Guin, S.B. Ogale, Starch (Tapioca) to carbon dots: an efficient green approach to an on–off–on photoluminescence probe for fluoride ion sensing, Analyst, 140 (2015) 1837–1841.
[37] S.C. Ray, A. Saha, N.R. Jana, R. Sarkar, Fluorescent carbon nano particles: synthesis, characterization, and bio imaging application, J. Phys. Chem. C., 113 (2009) 18546–14551.
[38] A. Iqbal, Y.J. Tian, X.D. Wang, D.Y. Gong, Y.L. Guo, K. Iqbal, Z.P. Wang, W.S. Liu, W.W. Qin, Carbon dots prepared by solid state method via citric acid and 1,10-phenanthroline for selective and sensing detection of Fe^{2+} and Fe^{3+}, Sensor. Actuat. B-Chem., 237 (2016) 408–415.
[39] S.M. Lu, G.L Li, Z.X Lv, N.N Qiu, W.H Kong, P.W Gong, G. Chen, L. Xia, X.X Guo, J.M You, Y.N Wu, Facile and ultra sensitive fluorescence sensor platform for tumor invasive bio maker β-glucuronidase detection and inhibitor evaluation with carbon quantum dots based on inner-filter effect, Biosens. Bioelectron., 85 (2016) 358–362.
[40] F.L. Zu, F.Y. Yan, Z.J. Bai, J.X. Xu, Y.Y. Wang, Y.C. Huang, X.G. Zhou, Working mechanisms and applications of the fluorescence quenching of carbon dots, Microchim. Acta, 184 (2017) 1899–1914.